

SCIENTIFIC DATA



OPEN

North American historical monthly spatial climate dataset, 1901–2016

DATA DESCRIPTOR

Heather MacDonald¹✉, Daniel W. McKenney², Pia Papadopol³, Kevin Lawrence⁴, John Pedlar⁵ & Michael F. Hutchinson⁶

We present historical monthly spatial models of temperature and precipitation generated from the North American dataset version “j” from the National Oceanic and Atmospheric Administration’s (NOAA’s) National Centres for Environmental Information (NCEI). Monthly values of minimum/maximum temperature and precipitation for 1901–2016 were modelled for continental United States and Canada. Compared to similar spatial models published in 2006 by Natural Resources Canada (NRCAN), the current models show less error. The Root Generalized Cross Validation (RTGCV), a measure of the predictive error of the surfaces akin to a spatially averaged standard predictive error estimate, averaged 0.94 °C for maximum temperature models, 1.3 °C for minimum temperature and 25.2% for total precipitation. Mean prediction errors for the temperature variables were less than 0.01 °C, using all stations. In comparison, precipitation models showed a dry bias (compared to recorded values) of 0.5 mm or 0.7% of the surface mean. Mean absolute predictive errors for all stations were 0.7 °C for maximum temperature, 1.02 °C for minimum temperature, and 13.3 mm (19.3% of the surface mean) for monthly precipitation.

Background & Summary

Climate data in North America are collected through a system of weather stations distributed unevenly throughout the continent. Practical uses often call for climate data far away from the meteorological stations. This need is filled by “spatially modelled” climate data that estimate climate values from historical weather observation networks. These spatial models are important in fields such as hydrology, horticulture, power generation and agriculture, among others. In particular, the monthly time step is highly useful. While for some applications, the daily timescale is preferable, monthly data sets typically have a lower prediction error, and can provide a useful alternative to researchers for whom daily data can quickly become computationally or otherwise unmanageable.

In this paper, we present updated historical monthly models of mean maximum and minimum temperature and total precipitation from 1901 to 2016, available at https://doi.org/10.26050/WDCC/CCH_3876085¹. The North American dataset (Northam version “j”)² was downloaded from the National Oceanic and Atmospheric Administration’s (NOAA’s) National Centres for Environmental Information. These data are publicly distributed at <https://data.nodc.noaa.gov/cgi-bin/iso?id=gov.noaa.ncdc:C00949>. We utilized ANUSPLIN³ to produce thin plate smoothing spline models of North American historical monthly mean values of daily minimum/maximum temperature and total precipitation from 1901 to 2016. McKenney *et al.*⁴ published similar models of these variables and ancillary bio-climate indices covering Canada and the United States (see also McKenney *et al.*⁵). We compare error estimates and surface diagnostics between the two sets of analyses, and report on features associated with the new models.

The current models are based on a greater number of stations compared to North American monthly historical spatial models published in 2006⁴. For the 2006 models, relatively few stations were available in the first half of

¹Natural Resources Canada – Canadian Forest Service, Great Lakes Forestry Centre, Research Scientist, P6A 2E5, 1219 Queen Street East, Sault Ste. Marie, Ontario, Canada. ²Natural Resources Canada – Canadian Forest Service, Great Lakes Forestry Centre, Chief, Landscape Analysis and Applications, P6A 2E5 1219 Queen Street East, Sault Ste. Marie, Ontario, Canada. ³Natural Resources Canada – Canadian Forest Service, Great Lakes Forestry Centre, Visiting Scientist, P6A 2E5 1219 Queen Street East, Sault Ste. Marie, Ontario, Canada. ⁴Natural Resources Canada – Canadian Forest Service, Great Lakes Forestry Centre, Geographical Information Systems Analyst, P6A 2E5 1219 Queen Street East, Sault Ste. Marie, Ontario, Canada. ⁵Natural Resources Canada – Canadian Forest Service, Great Lakes Forestry Centre, Forest Resource Biologist, P6A 2E5 1219 Queen Street East, Sault Ste. Marie, Ontario, Canada. ⁶Fenner School of Environment and Society, Australian National University, Canberra, Australia. ✉e-mail: heather.macdonald4@canada.ca

the 20th century; 1,221 stations were available from the U.S. Historical Climatology Network⁶, with an additional 46 stations for Alaska, and between 81 and 1742 stations from the Meteorological Service of Canada (from 1901 to 1993). The number of U.S. stations available in 2006 increased from over 5,000 stations between 1951 to over 7600 stations between 1971 and 2000.

The RTGCV, a measure of the predictive error akin to a spatially averaged standard predictive error estimate, averaged 0.94 °C for maximum temperature, 1.33 °C for minimum temperature, and 25.2% of the surface mean for precipitation from 1901 to 2016. RTGCVs for the current models were lower than those from 2006⁴ for maximum temperature (1.03 °C) and precipitation (>30%), and similar for minimum temperature (1.3 °C). MAEs (all stations) averaged 0.71 °C (minimum temperature), 1.02 °C (minimum temperature), and 13.31 mm, or 19.3% of the surface mean (precipitation). While differences exist in methodologies between the 2006 and current models, MAEs for precipitation were typically more than 30% of observed precipitation for the 2006 models, considerably larger than those presented in this study (under 20%).

Much of the improvement in the current models is due to efforts by NOAA and other agencies to rescue and restore historical temperature and precipitation records, as well as improved quality control processes. Northam “j” records, which have been subjected to a homogenization process, identified observations failing one or more quality control tests. The models presented in this paper also benefited from more systematic anomaly detection using studentized residuals. Despite these improvements, there are regional variations in model predictive accuracy, with coastal (Pacific and Atlantic) stations having the highest levels of predictive error for precipitation, particularly in the winter.

Methods

Source data. We used the North American Dataset (“Northam”) from the National Oceanic and Atmospheric Administration’s (NOAA’s) National Centres for Environmental Information². The Northam data are generated from the Global Historical Climate Network-Monthly (GHCN-M) dataset⁷. Northam has been the calibration dataset for the U.S. Historical Climate Network (USHCN) since version 2.

We downloaded version “j” of Northam. Northam version “j” values were subjected to a pairwise homogenization algorithm described in Menne and Williams⁸. The nature and quality of these homogenized data have been analysed in numerous published articles^{9–11}. GHCN-M quality control procedures are documented in Lawrimore *et al.*⁷. Observations flagged by NOAA through this process as having one or more quality control issues^{7,12} were dropped from our analysis¹³. A description of the GHCN quality data flags (“QFLAG”) is provided at <https://www1.ncdc.noaa.gov/pub/data/ghcn/daily/readme.txt>.

Figure 1 is a map of temperature and precipitation stations used for the analysis (see also¹³). Figure 2 illustrates the number of stations by variable by country by year. The number of Canadian precipitation station records increased from 528 in 1901 to over 2,000 stations from 1971 to 1993. The number of Canadian station records then declined to under 1,000 stations by 2012. In contrast, U.S. records increased from just over 3,000 in 1901 to over 8,000 from 1950 onwards.

Spatial modeling. We used thin plate smoothing spline algorithms as implemented in ANUSPLIN³. ANUSPLIN is a suite of FORTRAN programs under development for more than 25 years for applying thin plate spline data smoothing techniques to multi-variate data. ANUSPLIN has been used by researchers around the world^{14–16}. Here we only provide a brief description of thin plate splines. Readers are directed to Wahba¹⁷ for a more detailed description of thin plate splines. Hutchinson¹⁸ gives a general model for a thin plate spline function f fitted to n data values z_i at position x_i :

$$z_i = f(x_i) + \varepsilon_i (i = 1 \dots n)$$

in which the x_i refer to the independent variables, in this case, longitude, latitude and elevation multiplied by a factor of 100. Multiplying elevation by a factor of 100, which reflects the relative horizontal and vertical scales of atmospheric dynamics¹⁹, has been shown to improve predictive performance as demonstrated by Hutchinson²⁰ and Johnson *et al.*¹⁵. The ε_i are mean random errors that represent both measurement error as well as model deficiencies, reflecting localized effects below the resolution of the data network such as cold air drainage.

Precipitation values were subjected to a square root transformation prior to surface fitting. The square root transformation reduces skewness of the precipitation variable¹⁹, making the application of a fixed level of smoothing more consistent between small and large precipitation values across the data network. Tait *et al.*²¹ have confirmed that the square root transformation can yield a significant reduction in daily precipitation interpolation error. This transformation also makes the detection of data errors more consistent between small and large precipitation values.

The model solution was obtained by minimizing the generalised cross validation (GCV)⁴. The GCV is calculated by implicitly removing each data point and summing a suitably weighted square of the difference of each omitted data point from a surface fitted to all remaining data points¹⁷.

For large datasets, ANUSPLIN uses a sample of stations, called knots, to construct the thin plate smoothing spline surfaces. The use of knots reduces the computational complexity while still making use of every data point to calculate the fitted surface³. In this case, approximately 40% of data points were selected as knots.

In the course of modeling, we reviewed the signal, which is a diagnostic metric produced by ANUSPLIN. The signal statistic ranges between zero and the number of knots. Hutchinson and Gessler²² suggest that the signal should generally be no greater than about half the number of selected data points. Models with a good signal provide a balance between data smoothing and exact interpolation, while models with signals approaching the number of data points result in a rougher surface that approaches an exact interpolation of the source data. Exact interpolations reflect a model that is less robust, particularly in regions with few stations.



Fig. 1 Map of Northam “j” temperature (a) and precipitation (b) stations used for the current models (Mexican stations were not covered by the digital elevation model).

During the course of model development, root generalized cross validation (RTGCV) values in the log files output by ANUSPLIN’s SPLINE program were also reviewed. The RTGCV, the square root of the GCV described above, is an estimate of predictive standard error. Of note, the RTGCV is a conservative measure of standard error, because it includes data error as estimated by the ANUSPLIN program³.

ANUSPLIN flags data values that exceed a user-set threshold for studentized residuals, greatly improving the analyst’s ability to systematically detect anomalous recorded values and potential errors. For the current analysis, we examined flagged cases with a studentized residual of greater than 3.71. The probability of exceedance corresponds to a student’s t distribution²³. Following a comparison of flagged values against observations from neighbouring stations, we removed cases with studentized residuals exceeding 3.71; 0.05% of stations for minimum temperature, 0.15% for maximum temperature, and 0.17% for precipitation¹³. While these observations were not used to develop the gridded estimates, they were still retained to assess the quality of model predictions.

The CV estimates taken from SPLINE’s output point cross validation file were used to calculate the mean error (ME) statistics presented in this study, calculated as the cross-validation estimate less recorded station values. In addition, the mean absolute error (MAE) was calculated for a set of 160 stations¹³ for January, April, July, and October at 5-year intervals from 1905 to 2015. This set of stations was selected to reflect a representative and high quality sample compared to using all stations, which would under-represent northern stations. Please see <https://www1.ncdc.noaa.gov/pub/data/ghcn/daily/ghcnd-stations.txt> for a list of all GHCN stations (including those outside of North America) and their metadata.

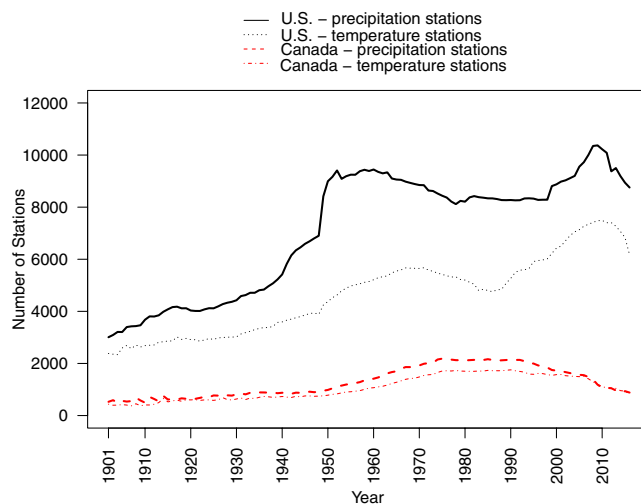


Fig. 2 Number of temperature and precipitation stations by year in Canada and in the United States.

Month	Northam “j” Models	2006 Models	Northam “j” Models	2006 Models	Northam “j” Models	2006 Models
	Maximum temperature (°C)		Minimum temperature (°C)		Precipitation (% of surface mean)	
January	0.96	1.01	1.40	1.41	25.7%	29.7%
February	0.93	1.00	1.37	1.40	26.3%	30.5%
March	0.91	0.99	1.25	1.24	24.9%	29.5%
April	0.92	1.00	1.19	1.15	24.8%	29.3%
May	0.95	1.04	1.22	1.17	25.0%	30.2%
June	0.99	1.11	1.29	1.21	26.9%	33.1%
July	1.03	1.14	1.36	1.27	29.3%	36.8%
August	1.00	1.12	1.40	1.32	29.7%	37.0%
September	0.94	1.05	1.43	1.37	27.9%	33.6%
October	0.88	0.96	1.40	1.40	26.1%	31.3%
November	0.89	0.93	1.34	1.34	24.7%	29.1%
December	0.93	0.97	1.36	1.36	24.9%	29.2%
Total	0.94	1.03	1.33	1.30	25.2%	31.6%

Table 1. Average RT GCV for monthly historical models by month based on Northam “j” (1901–2016) compared to 2006 models (McKenney *et al.*, 2006; 1901–2000).

As a final summary, MEs and MAEs were calculated for all stations by season (winter: December, January, and February; spring: March, April, and May; summer: June, July, and August; and autumn: September, October, and November). SAS software, Version 9.4 of the SAS System for Windows, was used to calculate differences between the predicted and recorded values, as well as to conduct correlation (PROC CORR) analyses on MEs and MAEs for the set of 160 test stations. Error maps were created in ArcGIS²⁴.

Data Records

Monthly grids of mean maximum/minimum temperature, and total precipitation were generated between 1901 and 2016 using a 60 arc-second (approximately 2 km) Digital Elevation Model covering the continental US and Canada are archived at the World Data Center for Climate (WDCC) at DKRZ¹. Post- 2016 grids are regularly published to the same DOI, and may also be obtained by contacting the corresponding author.

These monthly historical spatial models cover the geographic area from -168° to -52° longitude, and from 25° to 85° latitude from 1950 to 2016. Because of the small number of northern weather stations from 1901 to 1949, monthly historical models over this time cover a reduced area (-168° to -52° longitude, and from 25° to 60° latitude).

Technical Validation

Table 1 summarizes RTGCV statistics output from ANUSPLIN’s log files for monthly mean maximum/minimum temperature and total precipitation for current models as well as for those published in 2006⁴. RTGCVs for the current models are smaller for maximum temperature (0.94°C) and precipitation (25.2% of the surface mean) compared to the 2006 models (1.03°C and $>30\%$ respectively). The RTGCV for minimum temperature averaged 1.3°C , similar to the 2006 models.

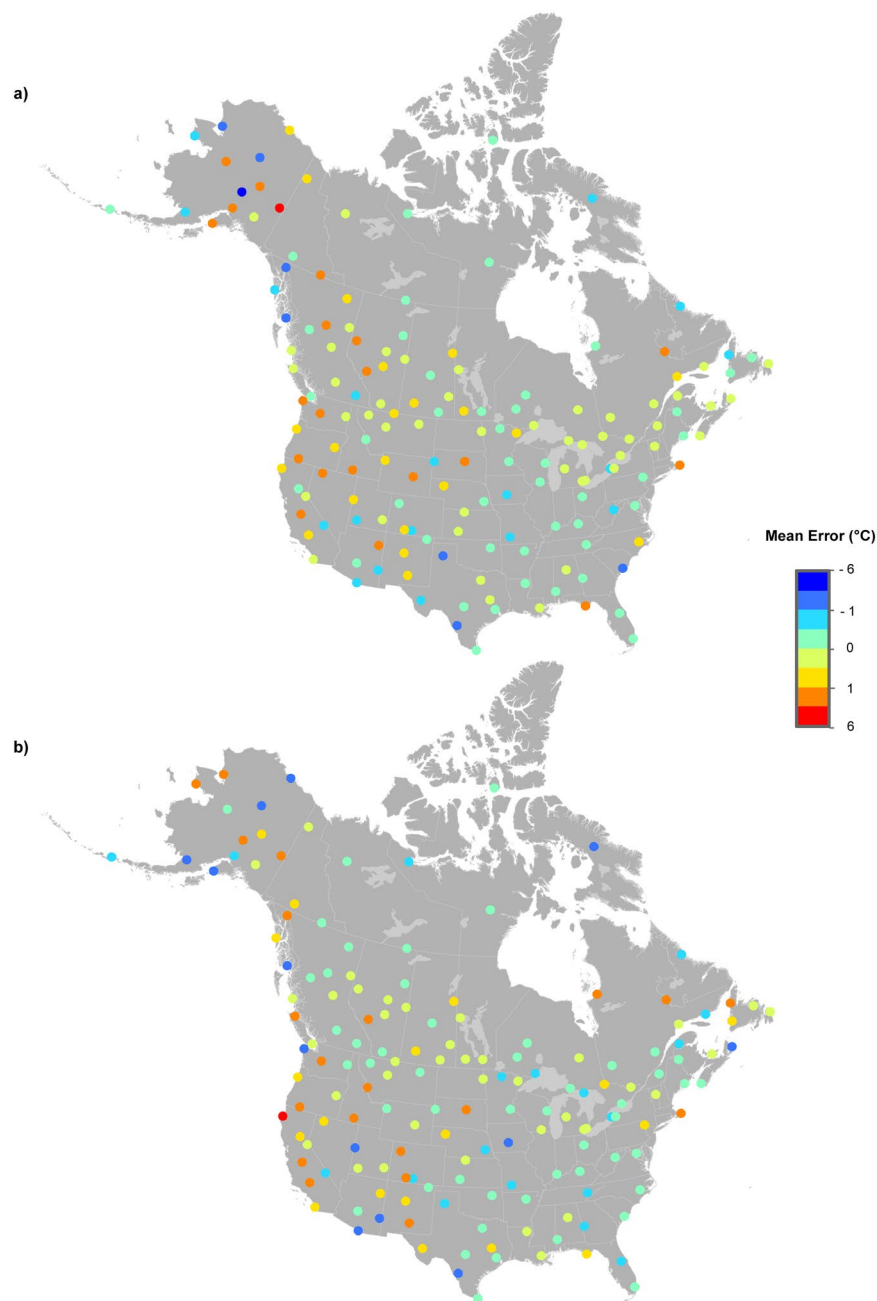


Fig. 3 Spatial variation in errors at 160 weather stations for maximum temperature ($^{\circ}\text{C}$). MEs were calculated by subtracting actual recorded values from estimates from 1950 to 2015 (every five years) for (a) January and (b) July.

The average RTGCV was 0.94°C for maximum temperature, lower than that for minimum temperature (1.33°C). The larger errors for minimum temperature are consistent with previous work and reflect shorter length scales and larger observational/representativeness errors for this variable compared to maximum temperatures. As noted by Hutchinson *et al.*¹⁸, maximum temperature patterns are strongly controlled by ground elevation intersecting linear atmospheric lapse rates but minimum temperature patterns are controlled by additional processes, including cold air drainage which inverts local lapse rates, particularly in winter months^{25,26}. Errors for maximum temperature are slightly larger in mid-summer, reflecting the greater variability of the higher temperature values¹⁹.

RTGCVs for minimum temperature ranged from 1.19°C in April to 1.4°C in October. RTGCVs for maximum temperature were largest in July (1.03°C) and lowest in October (0.88°C). For precipitation, the RTGCVs were largest in the summer (July and August), similar to the pattern reported by McKenney *et al.*⁴ This pattern reflects greater spatial complexity of convective rainfall compared to frontal precipitation occurring in winter months. Consistent with Hutchinson *et al.*¹⁹, we found lowest predictive errors in autumn for maximum temperature and precipitation, “consistent with the large well-organized synoptic systems that prevail in this season” (p. 725).

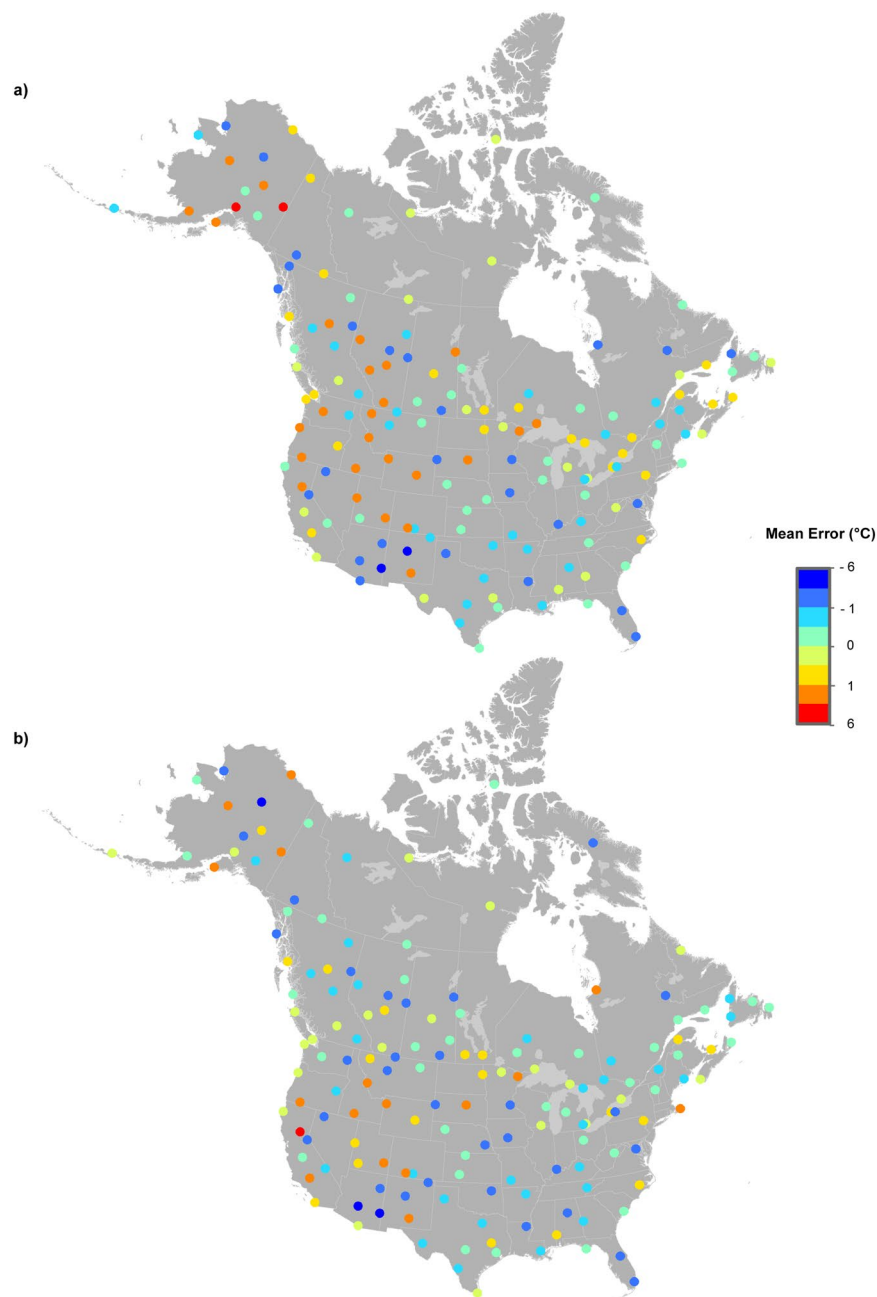


Fig. 4 Spatial variation in errors at 160 weather stations for minimum temperature ($^{\circ}\text{C}$). MEs were calculated by subtracting actual recorded values from estimates from 1950 to 2015 (every five years) for **(a)** January and **(b)** July.

The signal to number of knots ratio for the current models ranged between 47.0% and 64.7% for minimum temperature, and 39.5% to 60.0% for maximum temperature. For total monthly precipitation, the signal to knots ratio showed a wider range from 26.4% to 62.9%, but no problematic surfaces, as defined by Hutchinson & Gessler^{13,22}.

Figures 3 to 5 illustrate the MEs (Estimated less Recorded) and MAEs for January, April, July and October for 160 test stations every five years from 1905 to 2015. Maximum temperature model errors were typically between -3.0° and 3.0°C (Fig. 3). Minimum temperature predictive errors were larger than those for maximum temperature (Fig. 4). Model errors for total monthly precipitation (Fig. 5) were largest at the coasts in January. July precipitation errors were substantially smaller, falling mostly between ± 10 mm as compared to ± 50 mm for January precipitation errors. Larger model errors were evident along the Pacific and Atlantic coasts for January precipitation, linked to heavy and highly variable winter precipitation events.

Across the entire dataset, the MAE for maximum temperature was 0.71°C , compared to 1.02°C for minimum temperature. MAEs were largest in summer for maximum temperature, and in winter for minimum temperature as shown in Table 2. MAEs for precipitation were largest in the summer (21% of the surface mean) compared to

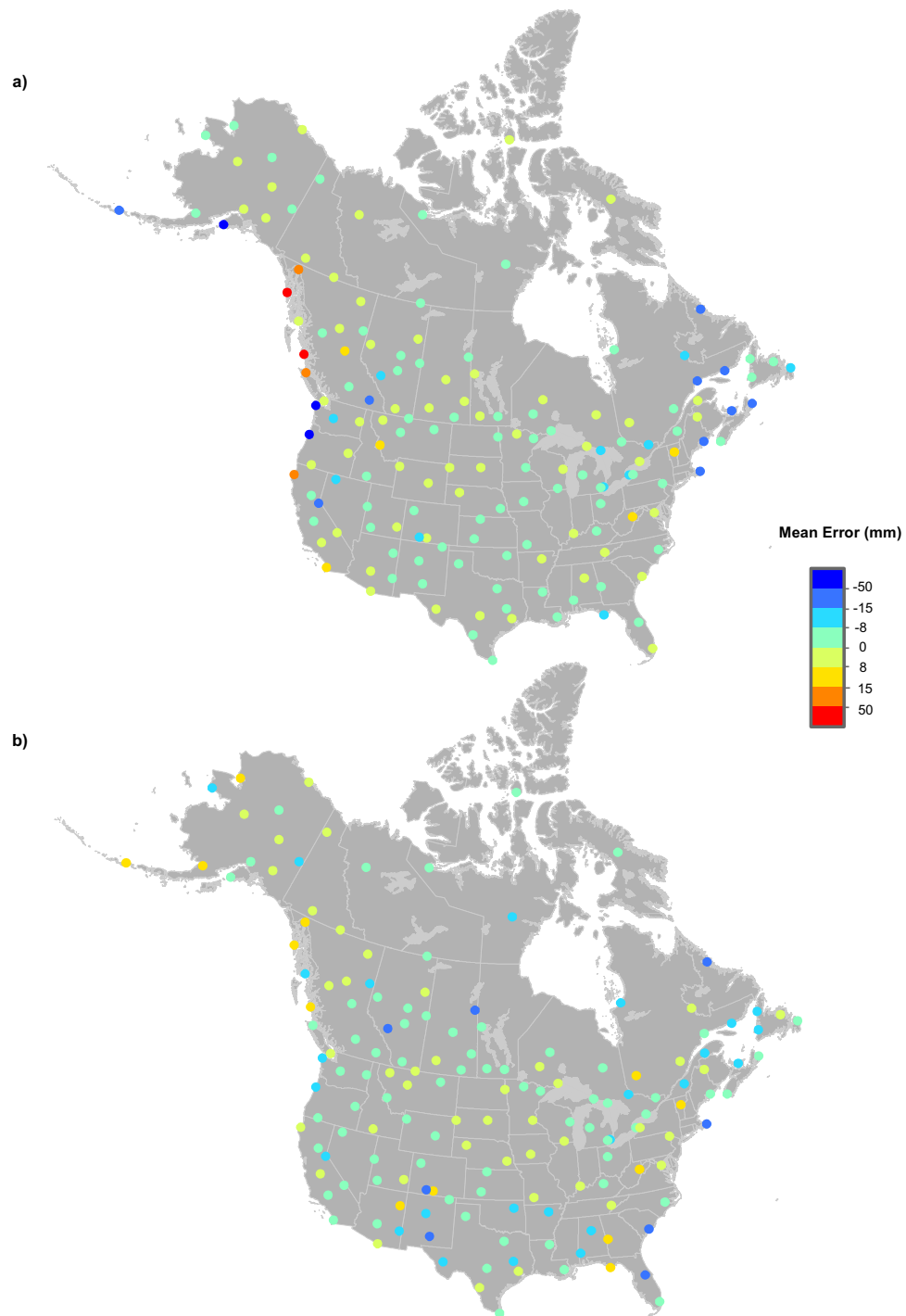


Fig. 5 Spatial variation in errors at 160 weather stations for total precipitation (mm). MEs were calculated by subtracting actual recorded values from estimates from 1950 to 2015 (every five years) for (a) January and (b) July.

spring (17.9%). The spatial models exhibited a negative (or dry) bias relative to recorded values for precipitation of 0.5 mm or 0.7% of the surface mean. In comparison, MEs for temperature variables were less than 0.01 °C.

Figure 6 illustrates the MEs (Estimated minus Recorded) and MAEs for January, April, July and October for 160 test stations every five years from 1905 to 2015. The MEs for maximum temperature models ranged between 0.0° and 0.3 °C (Fig. 5a), and from −0.3° to 0.1 °C for minimum temperature (Fig. 5b). The MAEs varied by year from 0.9° to 1.2 °C for minimum temperature, and from 0.5° to 0.9 °C for maximum temperature. MAEs showed a significant declining trend over time for April (maximum temperature), July (minimum temperature, maximum temperature), and October (maximum temperature), as shown in Table 3, suggesting an improvement in the quality of predictions over time. Temperature MEs were not significantly related to year (Table 4).

Season	Maximum temperature			Minimum temperature			Precipitation		
	Number of Observations	ME (°C)	MAE (°C)	Number of Observations	ME (°C)	MAE (°C)	Number of Observations	ME (mm)	MAE in mm (%)
Spring	5,606,375	0.007	0.71	5,548,625	0.0002	0.94	7,562,559	-0.44 (-0.6%)	12.57 (17.9%)
Summer	5,610,784	0.005	0.75	5,549,952	-0.003	1.01	7,572,416	-0.51 (-0.7%)	15.67 (21.0%)
Autumn	5,610,312	0.005	0.68	5,554,608	-0.004	1.05	7,570,562	-0.54 (-0.8%)	12.85 (19.3%)
Winter	5,602,647	0.002	0.74	5,548,834	-0.003	1.07	7,556,832	-0.52 (-0.8%)	12.04 (18.6%)
Total	22,430,118	0.005	0.72	22,202,019	-0.002	1.02	30,262,369	-0.50 (-0.7%)	13.31 (19.3%)

Table 2. Average cross-validation MAEs and MEs for the entire dataset by season and overall. Average MAEs/MEs were calculated by year and then averaged from 1901–2016. Total number of observations represents the sum of observations in each season or year (total).

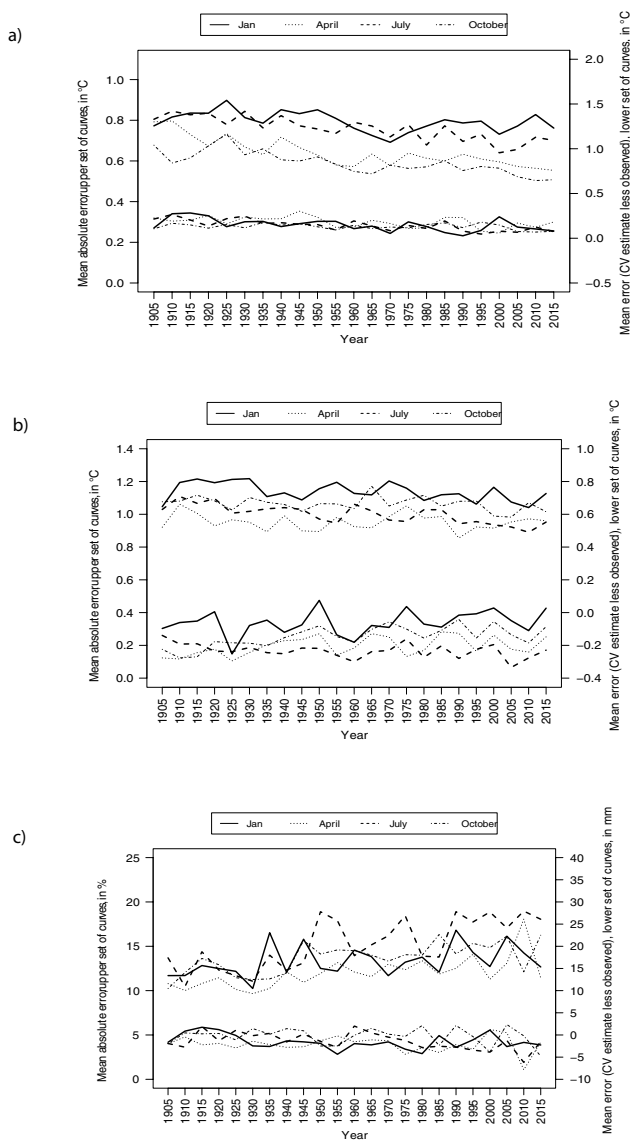


Fig. 6 Temporal variation in mean absolute error (left axis: upper set of curves on each graph) and bias (right axis; lower set of curves on each graph) for a set of 160 stations for (a) maximum temperature, (b) minimum temperature, and (c) precipitation. Error rates for January, April, July and October at five year intervals from 1905 to 2015 are plotted separately.

For precipitation, the MEs depicted in Fig. 6 ranged between -7.8 mm and 2.4 mm, or 9.7% to 19.0% of the precipitation surface mean. Precipitation MAEs (expressed as a percentage of the recorded value) were not significantly correlated with year (Table 3; see also <https://doi.org/10.17605/OSF.IO/2DAK5>). Precipitation MEs were

Variable	January	April	July	October
Maximum temperature	−0.026	−0.089*	−0.061*	−0.075*
Minimum temperature	−0.025	−0.006	−0.046*	−0.014
Precipitation	0.015	0.020	0.019	0.015

Table 3. Trend in MAEs (January, April, July, and October for the 160 test stations every five years from 1905, 1910... 2015). Values shown are the Pearson correlation coefficient (r) indicating the correlation between MAE and year. Starred values indicate statistically significant results at the 0.01 level. Temperature MAEs are expressed in °C and precipitation MAEs are expressed as a percentage of total monthly recorded precipitation.

Variable	January	April	July	October
Maximum temperature	−0.032	−0.035	−0.042	−0.013
Minimum temperature	−0.025	−0.006	−0.046	−0.014
Precipitation	−0.021	−0.012	−0.043*	−0.014

Table 4. Trend in MEs (January, April, July, and October for the 160 test stations every five years from 1905, 1910... 2015). Values shown are the Pearson correlation coefficient (r) indicating the correlation between ME and year. Starred values indicate statistically significant results at the 0.01 level. Temperature MEs are expressed in °C and precipitation MEs are expressed in mm.

not significantly correlated with year (Table 4), with the exception of July MEs which showed a significant declining trend over time. Cross-validation estimates and recorded values for the 160 test stations (every five years from 1905 to 2015) can be obtained from MacDonald¹³.

McKenney *et al.*⁴ assessed the 2006 models using a representative withheld sample of between 100 and 200 stations (increasing over the course of the century), which were not used in the creation of the spatial models. By comparison, the current study compared CV estimates to recorded values for 160 stations selected to be more representative than the full sample. We used a leave-one-out approach as opposed to withholding a set of stations simultaneously. We therefore urge some caution in directly comparing the MEs and MAEs between the two studies due to these methodological differences.

Usage Notes

The monthly historical spatial models presented in this manuscript will be of interest to researchers and practitioners that need historical estimates of temperature or precipitation variables for points or regions in North America. These temperature and precipitation estimates are central inputs to species richness²⁷, plant hardiness²⁸, forest productivity²⁹, forest cover change³⁰, carbon^{31,32}, water budget³³, and species distribution models³⁴, as well as in determining representativeness of different locations for conservation research³⁵. Further, models based on gauge data are also used as inputs to satellite-based precipitation estimates³⁶.

We note there are regional limitations associated with spatial models, especially for precipitation-related variables. Model predictions of precipitation along the coast were associated with larger errors, suggesting that a distance to coast independent variable might improve these estimates. For applications that exclusively include coastal areas of North America, more specialized gridded products may be more appropriate. However we note the paucity of station observations in some regions to develop/calibrate such models is especially problematic in Canada.

Code availability

SAS code used for data preparation and analysis has been published at Open Science Framework under the same name as the publication (<https://doi.org/10.17605/OSF.IO/2DAK5>)³⁷. SAS code and output for the residual analysis can be accessed from this DOI.

Received: 1 April 2020; Accepted: 27 October 2020;

Published online: 23 November 2020

References

- MacDonald, H. *et al.* North America Historical Monthly Spatial Climate Models, 1901–2016. *World Data Center for Climate (WDCC) at DKRZ* https://doi.org/10.26050/WDCC/CCH_3876085 (2020).
- Menne, M. J., Williams, C. N. Jr. & Korzeniewski, B. North American dataset. *NOAA National Centers for Environmental Information* <https://doi.org/10.7289/V5348HN5> (2017).
- Hutchinson, M., Xu, T. ANUSPLIN Version 4.4 User Guide. *The Australian National University, Fenner School of Environment and Society: Canberra, Australia*. <http://fenner.school.anu.edu.au/files/anusplin44.pdf> (2013).
- McKenney, D. W., Pedlar, J. H., Papadopol, P. & Hutchinson, M. F. The development of 1901–2000 historical monthly climate models for Canada and the United States. *Agric. For. Meteorol.* **138**, 69–81 (2006).
- McKenney, D. W. *et al.* Customized spatial climate models for North America. *Bull. Am. Meteorol. Soc.* **92**, 1611–1622 (2011).
- Karl, T., Williams, C. N., Quinlan, F. T. & Boden, T. A. *United States Historical Climatology Network (HCN) serial temperature and precipitation data*. (Carbon Dioxide Information Analysis Center, 1990).
- Lawrimore, J. H. *et al.* Global Historical Climatology Network-Monthly (GHCN-M); version 3. *NOAA National Centers for Environmental Information* <https://doi.org/10.7289/V5X34VDR> (2011).
- Menne, M. J. & Williams, C. N. Jr. Homogenization of temperature series via pairwise comparisons. *J. Clim.* **22**, 1700–1717 (2009).

9. Williams, C. N., Menne, M. J. & Thorne, P. W. Benchmarking the performance of pairwise homogenization of surface temperature in the United States. *J. Geophys. Res.: Atmos.* **117**, 1–16 (2012).
10. Vose, R. S. *et al.* Improved historical temperature and precipitation time series for U.S. climate divisions. *J. Appl. Meteorol. Clim.* **53**, 1232–1251 (2014).
11. Hausfather, Z., Cowtan, K., Menne, M. J. & Williams, C. N. Evaluating the impact of U.S. historical climatology network homogenization using the U.S. climate reference network. *Geophys. Res. Lett.* **43**, 1695–1701 (2016).
12. Gleason, B., Williams, C., Menne, M. & Lawrimore, J. *Modifications to GHCN-Monthly (version 3.3. 0) and USHCN (version 2.5. 5) processing systems*. Report No. GHCNM-15-01 (NOAA NCEI, 2015).
13. MacDonald, H. *et al.* North American historical monthly spatial climate dataset, 1901–2016. *figshare* <https://doi.org/10.6084/m9.figshare.c.5095481> (2020).
14. Li, W., Li, X., Tan, M. & Wang, Y. Influences of population pressure change on vegetation greenness in China's mountainous areas. *Ecol. Evol.* **7**, 9041–9053 (2017).
15. Johnson, F. & Hutchinson, M. The, C., Beesley, C. & Green, J. Topographic relationships for design rainfalls over Australia. *J. Hydrol.* **533**, 439–451 (2016).
16. Fick, S. E. & Hijmans, R. J. WorldClim 2: new 1-km spatial resolution climate surfaces for global land areas. *Int. J. Climatol.* **37**, 4302–4315 (2017).
17. Wahba, G. *Spline models for observational data*. Vol. 59 (Siam Publications, 1990).
18. Hutchinson, M. F. Interpolating mean rainfall using thin plate smoothing splines. *Int. J. GIS* **9**, 385–403 (1995).
19. Hutchinson, M. F. *et al.* Development and testing of Canada-wide interpolated spatial models of daily minimum-maximum temperature and precipitation for 1961–2003. *J. Appl. Meteorol. Clim.* **48**, 725–741 (2009).
20. Hutchinson, M. F. Interpolation of rainfall data with thin plate smoothing splines. Part II: Analysis of topographic dependence. *J. Geogr. Inform. Decis. Anal.* **2**, 152–167 (1998).
21. Tait, A., Henderson, R., Turner, R. & Zheng, X. Thin plate smoothing spline interpolation of daily rainfall for New Zealand using a climatological rainfall surface. *Int. J. Climatol.: J. Royal Meteorol. Soc.* **26**, 2097–2115 (2006).
22. Hutchinson, M. & Gessler, P. Splines—more than just a smooth interpolator. *Geoderma* **62**, 45–67 (1994).
23. Kutner, M. H., Nachtsheim, C. J., Neter, J. & Li, W. *Applied linear statistical models*. Vol. 103 (McGraw-Hill Irwin Boston, 2005).
24. Environmental Systems Research Institute (ESRI). *ArcGIS Desktop Release 10. (Redlands, California)* (2011).
25. Daly, C., Conklin, D. R. & Unsworth, M. H. Local atmospheric decoupling in complex topography alters climate change impacts. *Int. J. Climatol.* **30**, 1857–1864 (2010).
26. Holden, Z. A., Crimmins, M. A., Cushman, S. A. & Littell, J. S. Empirical modeling of spatial and temporal variation in warm season nocturnal air temperatures in two North Idaho mountain ranges, USA. *Agric. For. Meteorol.* **151**, 261–269 (2011).
27. Marshall, K. E. & Baltzer, J. L. Decreased competitive interactions drive a reverse species richness latitudinal gradient in subarctic forests. *Ecology* **96**, 461–470 (2015).
28. McKenney, D. W. *et al.* Change and evolution in the plant hardiness zones of Canada. *BioScience* **64**, 341–350 (2014).
29. Rahimzadeh-Bajgiran, P., Hennigar, C., Weiskittel, A. & Lamb, S. Forest potential productivity mapping by linking remote-sensing-derived metrics to site variables. *Remote Sens.* **12**, 2056 (2020).
30. Carpino, O. A., Berg, A. A., Quinton, W. L. & Adams, J. R. Climate change and permafrost thaw-induced boreal forest loss in northwestern Canada. *Environ. Res. Lett.* **13**, 084018 (2018).
31. Holmberg, M. *et al.* Ecosystem services related to carbon cycling – modeling present and future impacts in boreal forests. *Front. Plant Sci.* **10**, 343 (2019).
32. Packalen, M. S., Finkelstein, S. A. & McLaughlin, J. W. Climate and peat type in relation to spatial variation of the peatland carbon mass in the Hudson Bay Lowlands, Canada. *J. Geophys. Res.: Biogeosciences* **121**, 1104–1117 (2016).
33. Wang, S., McKenney, D. W., Shang, J. & Li, J. A national-scale assessment of long-term water budget closures for Canada's watersheds. *J. Geophys. Res.: Atmos.* **119**, 8712–8725 (2014).
34. Wang, Y., Casajus, N., Buddle, C., Berteaux, D. & Larrivée, M. Predicting the distribution of poorly-documented species, Northern black widow (*Latrodectus variolus*) and Black purse-web spider (*Sphodros niger*), using museum specimens and citizen science data. *PLoS One* **13**, e0201094 (2018).
35. Zhou, T. *et al.* Coupling between plant nitrogen and phosphorus along water and heat gradients in alpine grassland. *Sci. Total Environ.* **701**, 134660 (2020).
36. Hermosilla, T. *et al.* Mass data processing of time series Landsat imagery: pixels to data products for forest monitoring. *Int. J. Digit. Earth* **9**, 1035–1054 (2016).
37. MacDonald, H. *et al.* North American Historical Monthly Spatial Climate Dataset, 1901–2016. *Open Science Framework* <https://doi.org/10.17605/OSF.IO/2DAK5> (2020).

Acknowledgements

The authors gratefully acknowledge the insightful comments of two anonymous reviewers that greatly improved the manuscript. We would like to thank Kaitlin de Boer for producing the maps. Also, we are greatly indebted to multiple representatives of NOAA/NCEI for providing us with Northam “j” data. We also acknowledge funding provided to the Economic Analysis and Geo-spatial Tools Group of Natural Resources Canada - Canadian Forest Service, Great Lakes Forestry Centre by Environment and Climate Change Canada.

Author contributions

Heather MacDonald, primary analyst and author, Dan McKenney, significant contribution to the report and interpretation of results, originator of the project, John Pedlar, significant contribution to the report and interpretation of results, particularly in comparing model results to previously published models, Pia Papadopol, implementation of ANUSPLIN models, quality control, and review of final products, Kevin Lawrence, implementation of ANUSPLIN models, quality control, and review of final products Michael F. Hutchinson, ANUSPLIN creator, review of model results and final products.

Competing interests

Funding was provided to the Economic Analysis and Geospatial Tools Group of Natural Resources Canada – Canadian Forest Service, Great Lakes Forest Service by Environment and Climate Change Canada (ECCC). However, these models were developed independently by the authors of this paper

Additional information

Correspondence and requests for materials should be addressed to H.M.

Reprints and permissions information is available at www.nature.com/reprints.

Publisher's note Springer Nature remains neutral with regard to jurisdictional claims in published maps and institutional affiliations.



Open Access This article is licensed under a Creative Commons Attribution 4.0 International License, which permits use, sharing, adaptation, distribution and reproduction in any medium or format, as long as you give appropriate credit to the original author(s) and the source, provide a link to the Creative Commons license, and indicate if changes were made. The images or other third party material in this article are included in the article's Creative Commons license, unless indicated otherwise in a credit line to the material. If material is not included in the article's Creative Commons license and your intended use is not permitted by statutory regulation or exceeds the permitted use, you will need to obtain permission directly from the copyright holder. To view a copy of this license, visit <http://creativecommons.org/licenses/by/4.0/>.

The Creative Commons Public Domain Dedication waiver <http://creativecommons.org/publicdomain/zero/1.0/> applies to the metadata files associated with this article.

© Crown 2020